J. theor. Biol. (1987) **129**, 17–39

Paddles and Rakes: Fluid Flow Through Bristled Appendages of Small Organisms

A. Y. L. CHEER

Department of Mathematics, University of California, Davis, CA 95616, *U.S.A.*

AND

M. A. R. KOEHL

Department of Zoology, University of California, Berkeley, CA 94720, *U.S.A.*

(*Received* 4 *July* 1986, *and in revised form* 2 *June* 1987)

Many small organisms capture food particles, locomote through water or air, or create currents using appendages bearing arrays of long bristles. The performance of these arrays of hairs depends on the movement of fluid relative to them. We have modeled the fluid flow around such hairs, and have used the model to predict, for a range of biologically-relevant circumstances: (1) the steepness of the shear gradients adjacent to the hairs, (2) the leakiness of the gaps between pairs of hairs, and (3) the drag force on hairs with neighbors. We point out the circumstances under which bristled appendages function as rakes versus those under which they operate as paddles. Our results suggest that a simple change in size or speed of a bristled appendage can lead to a novel mode of functioning under some circumstances, whereas in other situations differences in morphology or behavior have little effect on performance.

Introduction

Many organisms move bristled appendages through the water or air around them. Among the numerous examples of bristled feeding appendages are the particle-capturing structures of such ecologically important planktonic animals as euphausids, cladocerans, and copepods, and of abundant benthic organisms such as barnacles. In addition, many organisms other than crustaceans use arrays of cylindrical structures to catch particulate food, including some heterotrophic microflagellates and aquatic insect larvae. Numerous planktonic organisms also use bristled appendages to locomote or to produce water currents. Furthermore, there are many examples of bristled structures used in air, such as the feather-like antennae of moths and the hairy (rather than membranous) wings of very small insects. If we are to understand the mechanisms by which these arrays of cylindrical bristles move fluids and catch particles, we must first elucidate some of the basic patterns of fluid behavior when groups of cylinders move through it.

Most of the setae, setules, and other biological fibers mentioned above and listed in Table 1 operate at Reynolds numbers of the order of 10^{-5} to 1. Reynolds number ($\mathrm{Re} = UL/\nu$, where U is velocity, L is a linear dimension (in this case the diameter of the cylinder), and ν is the kinematic viscosity of the fluid) represents the ratio

0022-5193/87/210017+23 $3.00/0

TABLE 1

Organism	Structure	Fluid[a]	Cylinder diameter (μm)	Width of gap (μm)	U_s ($m.s^{-1}$)	Re	References
Similium vittatum (black fly, aquatic larva)	cephalic fan: rays	fw	5**[b]	30 to 50**[b]	0·18* to 0·8**	0·9 to 4	* Craig & Chance (1982) ** Ross & Craig (1980)
	microtrichia		0·2**[b]	0·15**[b]	0·18* to 0·8**	0·2 to 4×10^{-2}[c]	
Eucalanus pileatus (calanoid copepod)	first maxilla:	sw					* Koehl & Strickler (1981) ** Koehl, unpubl. data
	setae		7**	24**	$1{\cdot}5\times10^{-2}$*	0·1	
	setules		2**	4**	$1{\cdot}5\times10^{-2}$*	3×10^{-2}[c]	
	maxilliped:						
	setae		10**	26*	$2{\cdot}4\times10^{-2}$	0·2	
Centropages typicus (calanoid copepod)	maxilliped:	sw					* Koehl & Strickler (1981) ** Koehl, unpubl. data
	setae		3·6**	26*	$3{\cdot}9\times10^{-2}$	0·1	
Euphausia superba (krill)	sixth periopod:	sw					McClatchie & Boyd (1983)
	1° setae		4·5[b]	34 to 58	4×10^{-2} to $2{\cdot}5\times10^{-1}$	0·1 to 0·6	
	2° setae		0·6[b]	6·5 to 9·3	4×10^{-2} to $2{\cdot}5\times10^{-1}$	1×10^{-2} to 8×10^{-2}[c]	
	3° setae		0·3[b]	1·2[b]	4×10^{-2} to $2{\cdot}5\times10^{-1}$	6×10^{-3} to 4×10^{-2}[c]	
Meganyctiphanes norvegica (krill)	sixth periopod:	sw					McClatchie & Boyd (1983)
	1° setae		14[b]	71[b]	3×10^{-3} to 9×10^{-3}	7×10^{-2} to 2×10^{-1}	
	2° setae		1·2[b]	23[b]	3×10^{-3} to 9×10^{-3}	2×10^{-3} to 6×10^{-3}[c]	
	3° setae		0·4[b]	5·3[b]	3×10^{-3} to 9×10^{-3}	6×10^{-4} to 2×10^{-3}[c]	
Encarsia formosa (small wasp)	wing:	air					Ellington (1975)
	marginal hairs		2	11	0·5	7×10^{-2}	

Thrips physapus (small insect)	forewing: "cilia" (hairs):	air					* Ellington (1980) ** Kuethe (1975)
	of ventral fringe		2*	20*	(not given)	$\sim 1\times10^{-2}$ **	
	of trailing fringe		1*	12*	(not given)	$\sim 1\times10^{-2}$ **	
Daphnia magna (cladoceran)	3rd thoracic appendage: setae	fw	3·5	5[b]	$1{\cdot}6\times10^{-3}$ to $3{\cdot}1\times10^{-3}$ [d]	5×10^{-3} to 1×10^{-2}	Gerritsen & Porter (1982)
	setules		0·4	1·0	$1{\cdot}6\times10^{-3}$ to $3{\cdot}1\times10^{-3}$ [d]	6×10^{-4} to 1×10^{-3} [c]	
Daphnia carcinata (cladoceran)	3rd thoracic appendage: setules	fw	0·29	0·23	(not given)	1×10^{-3} to 4×10^{-3}	Ganf & Shiel (1985)
Daphnia parvula (cladoceran)	3rd thoracic appendage: setae	fw	1·8[b]	5[b]	$1{\cdot}5\times10^{-4}$ [d]	3×10^{-4}	Gerritsen & Porter (1982)
	setules		0·32	0·36	$1{\cdot}5\times10^{-4}$ [d]	5×10^{-5} [c]	
Bosmina longirostris (cladoceran)	3rd thoracic appendage: setae	fw	2[b]	16[b]	$2{\cdot}9\times10^{-4}$ [d]	6×10^{-4}	Porter *et al.* (1983)
	setules		0·36	0·62	$2{\cdot}9\times10^{-4}$ [d]	1×10^{-4} [c]	
Ceriodaphnia lacustrus (cladoceran)	3rd thoracic appendage: setae	fw	0·7[b]	3·1[b]	$1{\cdot}6\times10^{-4}$ [d]	1×10^{-4}	Porter *et al.* (1983)
	setules		0·15	0·25	$1{\cdot}6\times10^{-4}$ [d]	2×10^{-5}	
Actinomonas mirabilis (protozoan)	pseudopodia	sw	0·2	1 to 3	$1{\cdot}3\times10^{-4}$	2×10^{-5}	Fenchel (1982)
Cyclidium sp. (protozoan)	paraoral membrane: cilia	sw	0·2	0·3	5×10^{-5}	1×10^{-5}	Fenchel (1980)
Monosiga sp. (protozoan)	pseudopodia	sw	0·1	0·3	1×10^{-5} to $1{\cdot}5\times10^{-5}$	1×10^{-6}	Fenchel (1982)

[a] fw = freshwater, $\nu = 1{\cdot}004\times10^{-6}$ m^2 . s^{-1} at 20°C; sw = seawater, $\nu = 1{\cdot}047\times10^{-6}$ m^2 . s^{-1} at 20°C and $1{\cdot}837\times10^{-6}$ m^2 . s^{-1} at 0°C; air, $\nu = 1{\cdot}5\times10^{-5}$ m^2 . s^{-1} at 20°C.
[b] Measured on a published photograph.
[c] Calculated using U_∞. (The true Re would be lower because the flow encountered by these small bristles is slowed by the larger hairs to which they are attached.)
[d] Calculated from reported frequency and arc of appendage flapping.

of inertial forces to viscous forces for a particular flow situation. Hence, viscosity is more important than inertia in determining the flow around these biological cylinders. Whenever a viscous fluid flows over a solid surface, the layer of fluid in contact with the surface sticks to it and a shear gradient exists between the surface and the freestream flow. The lower the Re, the thicker this shear gradient layer is with respect to the dimensions of the object. The same is true for a hair moving through a stationary fluid—some fluid sticks to and moves along with the bristle, and a shear gradient exists in the fluid around it.

The amount of fluid moving with bristles affects a number of important biological processes such as feeding, locomotion, and chemoreception. Consider, for instance, just one of these examples: the flow around hairs determines the mechanisms that organisms with bristled appendages can use to catch particulate food. If shear gradients are thick around setae, they can't reach out and grab a food particle because the particle is pushed away by the water moving with the setae (e.g. Koehl & Strickler, 1981). Furthermore, if little fluid moves through the spaces between the setae on an appendage, how effective can that structure be as a sieve to strain particles from the fluid? In addition, the steepness of the shear gradient next to a fiber affects the ability of the fiber to filter particles out of the surrounding water by mechanisms other than sieving (e.g. Davies, 1973; Speilman, 1977). Some setulated appendages may function as the rakes, sieves, and scoop-nets that they resemble in structure, whereas others may operate more like paddles that move parcels of water containing food. A debate has grown in the biological literature about whether or not the setulose appendages of certain ecologically important planktonic animals operate as leaky sieves or as paddles (for example, cladocerans, e.g. Gerritsen and Porter, 1982; Porter *et al.*, 1983; Ganf and Shiel, 1985; Brendelberger *et al.*, 1986; copepods, see e.g. the review by Koehl, 1984; Price and Paffenhöfer, 1986).

In this paper we present a mathematical description of fluid motion with respect to cylinders (e.g. bristles, setae, hairs) at a variety of biologically relevant sizes, spacings, and velocities. Our purpose is to explore the circumstances under which the setulose appendages of small organisms are functionally paddles and those under which they act like leaky rakes. We also investigate the drag on setae, and hence the mechanical load they structurally must bear. The intent of this paper is to present some general predictions of the model and to outline broadly their biological implications. Elsewhere we consider cases of specific organisms, utilizing results of this model as well as empirical data (moths and black fly larvae: Cheer & Koehl, 1987, copepods: Koehl & Cheer, in prep.).

The Model

We consider here the case of appendages bearing a finite number of hairs; many examples of such appendages can be found among planktonic crustaceans. Water is free to move around the sides of the setae on such appendages as well as to move through the spaces between neighboring setae. Therefore, it is *not* appropriate to model such setae as an infinite row of cylinders between which all the fluid is forced to move (e.g. Tamada & Fujikawa, 1957; Miyagi, 1958). Rather, as a first approximation to the flow in the vicinity of setae on an appendage of finite width, we consider

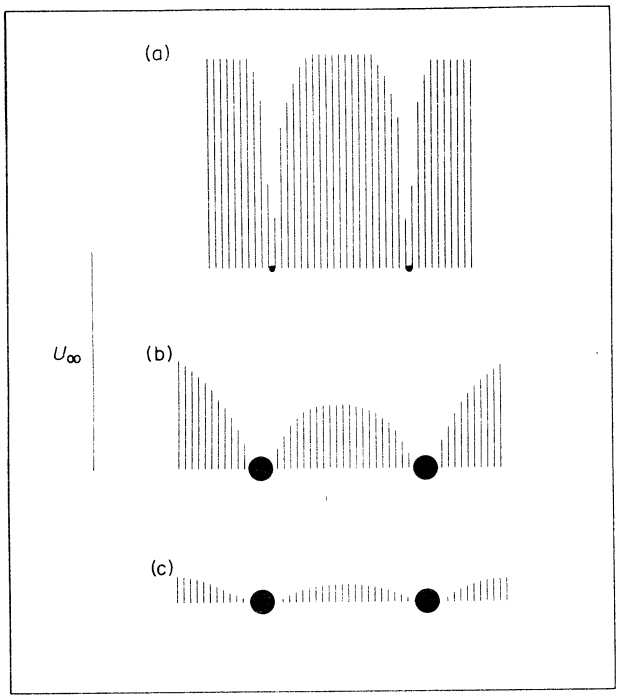

FIG. 1. Examples of fluid motion with respect to a pair of circular cylinders (shown as black circles). The lines represent the velocity vectors in the y direction (see Fig. A1). Note that the vectors are all drawn to the same scale with respect to the freestream velocity (U_∞, shown by the line to the left of the figure), although the U_∞'s in each example are quite different from each other. (a) A pair of cylinders 0·1 μm in diameter operating at a Re of 10^{-1} with a gap between them of 5 μm. (b) A pair of cylinders of the same Re and spacing as in (a), but 1 μm in diameter. (c) A pair of cylinders of the same diameter and spacing as in (b), but operating at a Re of 10^{-5}.

the flow around and between a two-dimensional cross-section of a pair of circular cylinders (Fig. 1). We consider the case where the direction of motion is perpendicular to the line intersecting the centers of both cylinders.

The flow fields around pairs of cylinders were calculated as described in Appendix 1. Calculations were done for cylinders 1 μm and 0.1 μm in diameter operating at Re's of 10^{-5} to 0·5. The width of the gap between the cylinders varied between 0·3 μm and 50 μm. These values were chosen to represent a range of biological setae, hairs, and bristles for which the appropriate data could be found in the literature (see Table 1). Flow fields around isolated cylinders of the same Re's were also calculated using solutions to the Oseen and Stokes equations.

A simpler alternative approach to modeling the flow through a setulose appendage is to treat the appendage as a porous plate. This approach is outlined in Appendix 2, as are our reasons for preferring the two-cylinder model.

Shear Gradients Near Moving Cylinders

The steepness of the shear gradient near a hair can affect a number of biological processes. If the hair is involved in filtering particulate food from the water, the flow field in its vicinity can affect the efficiency of capture of particles of various

characteristics (e.g. Davies, 1973; Speilman, 1977). The shear gradient near the seta can also affect the flux of dissolved materials to its surface (e.g. Gavis, 1976), which in turn can affect processes such as chemoreception and gas exchange. The shear gradient around a cylinder also affects the deflection of any mechanosensory bristles it may bear.

Some examples of flow fields around pairs of hairs are illustrated in Fig. 1. It can be seen that the steepness of the shear gradients in the fluid near the setae can be quite different under various circumstances.

One simple measure of the steepness of the shear gradient near a hair is the velocity ratio u_x/U_∞, where u_x is the fluid velocity with respect to the seta in the y direction at some point x near the surface of the seta, and U_∞ is the free-stream velocity with respect to the seta (see Fig. A1). The higher this velocity ratio, the less fluid at point x is being moved along with the seta and the steeper the shear gradient is along the surface of the seta. The velocity ratio varies between zero (where the fluid at x is moving along with the seta at the same velocity as the seta) to one (where x is outside the shear gradient and is not moved as the seta passes by). An example of how velocity ratio varies with spacing between neighboring bristles and with their Re is illustrated in Fig. 2. These results indicate a number of biologically interesting features of flow around hairs:

(1) As Re increases, the velocity ratio increases. At the higher end of the Re range examined, little fluid is dragged along with the setae and the shear gradients around them are steep. In contrast, at very low Re's, much water is dragged along

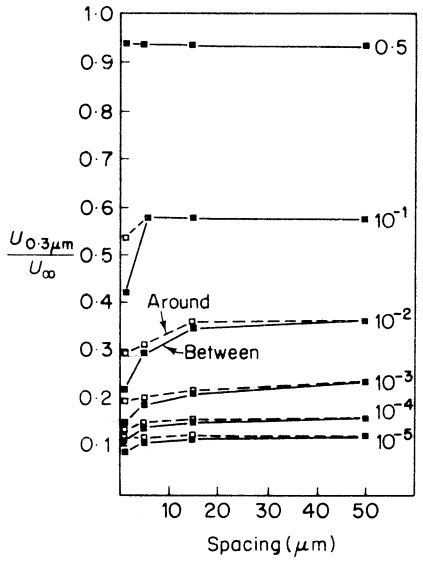

FIG. 2. Ratio of velocity at a point 0·3 μm from the surface of a cylinder ($U_{0\cdot3\mu m}$) to the free-stream velocity (U_∞), plotted vs. the width of the gap between neighboring cylinders. Numbers at the right end of each curve indicate the Re (based on cylinder diameter); in this example the cylinders are 1·0 μm in diameter. Solid lines represent flow between a pair of cylinders; dashed lines represent flow around the outside of a pair of cylinders.

with the setae, shear gradients are gentle, and the shear gradients can be thicker than the space between neighboring hairs.

(2) If an organism changes the velocity of its appendages (i.e. changes the Re), this will have a bigger effect on velocity ratio at the upper end of the Re range examined. This means that for organisms whose hairs operate at very low Re's, changes in the speed of movement of a finite group of bristles will have little effect on the steepness of the shear gradients around them. In contrast, for organisms whose hairs operate at Re's of about 10^{-2} to 0·5, changing speed can be a mechanism of changing how much fluid is dragged along with the setae.

(3) As a pair of setae are moved closer together, the velocity ratio decreases, especially when the inter-setal distance is already small. This effect is most pronounced at Re's of the order of 10^{-2}. For setae operating at very low Re's, the shear gradient is so gradual and so thick that a change in spacing doesn't make much difference to the velocity at a point, even when the hairs are quite far apart. For setae operating at Re's approaching one, a neighbor doesn't have much effect, even when quite close, hence a change in spacing again doesn't make much difference to the velocity at a point. This suggests that, for setulose appendages of finite width, the spacing between neighboring hairs will have little effect on those aspects of performance that depend on shear gradients near the hairs *if* they operate at very low Re's or at Re's approaching 1. In contrast, the performance of setulose appendages operating at Re's of order 10^{-2} would be expected to change as a function of intersetal spacing.

(4) Flow at a given distance from a seta is slower between adjacent setae than it is around their outer sides. Not surprisingly, this difference in flow between vs. around a pair of hairs becomes pronounced as the spacing between them is reduced. The greatest effect that a change in spacing produces on this difference in flow occurs at Re's in the middle of the range examined. Thus, again we would expect that if intersetal spacing has an effect on performance, that effect would be seen for organisms whose hairs operate at Re's of order 10^{-2}.

(5) The patterns described above are evident for setae both of 0·1 μm diameter and of 1 μm diameter, although in the latter case the velocity ratios are lower for the given Re's and spacings (which is not surprising since, to operate at a given Re, the wide hairs must move more slowly than the slim hairs). Nonetheless, as illustrated in Fig. 3, for a given width of space between adjacent setae moving at a given *speed* U_x, slimmer setae do have slightly faster flow between them than do wider hairs. This difference is somewhat more pronounced if the appendage is moving rapidly.

The width of a row of bristles may affect the shear gradients that develop in the fluid near them. This effect is due to the difference in the behavior of fluid near a finite array of hairs (as examined here) and that of fluid near an infinite array (as examined by e.g. Tamada & Fujikawa, 1957). In the case of an infinite array, the fluid is forced to move between the hairs and the shear gradients become steeper as the hairs are moved closer together. In contrast, when fluid is free to move around the outside of a pair of hairs, the shear gradient between the hairs becomes *less* steep as they are moved closer together. Thus, we might expect shear gradients in the mid-region of a setulose appendage to be greater than we have predicted here

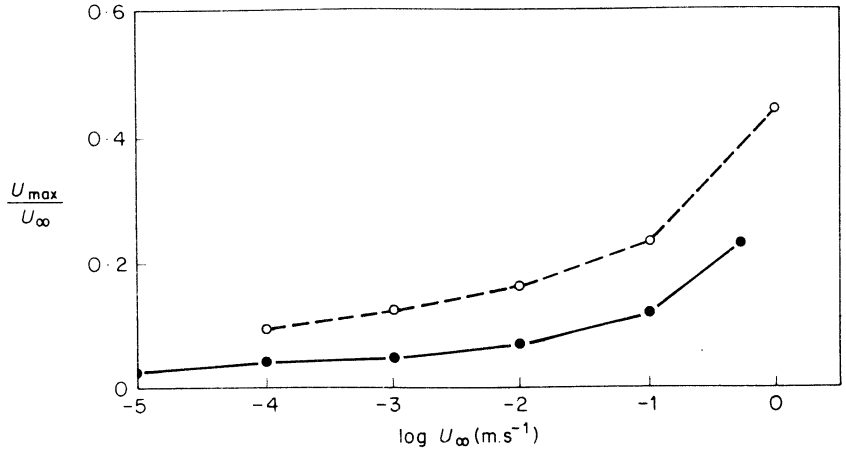

FIG. 3. Ratio of the maximum velocity (U_{max}) reached at the midpoint between a pair of cylinders to the free-stream velocity (U_∞), plotted vs. the log of the free-stream velocity (U_∞). In this example, the cylinders are separated by a space that is 1 μm wide. The dashed line shows results for cylinders 0·1 μm in diameter, and the solid line for cylinders 1 μm in diameter.

if the row of setae is wide enough that it is more difficult for fluid in the mid-region to move around the edges than to move through the intersetal gaps. This suggests that the effect on local shear gradients of the width of an entire array of bristles is an important area to investigate (in addition to the effects of bristle diameter and spacing examined here) if we are to understand the functional morphology of setulose structures.

Leakiness of Bristled Appendages: Paddles vs Rakes

While the velocity ratio is a measure of the steepness of the shear gradient next to a seta, a better measure of the degree to which the appendage operates as a rake vs. as a paddle is its "leakiness". We define leakiness here as the ratio of the volume of fluid that actually moves between a pair of setae to the volume across which that setal pair sweeps in a unit of time (Fig. 4). We have determined the volume of fluid

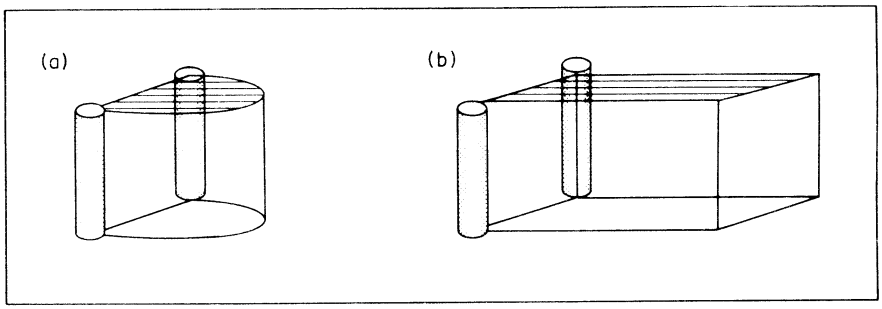

FIG. 4. Leakiness is defined here as the ratio of the volume of fluid that actually moves between a pair of cylinders of unit length in a unit of time (shown in (a)), to the volume between the cylinders across which they sweep in that unit of time (shown in (b)).

moving between a pair of hairs of unit length by taking the area of the velocity profile between them. The leakiness of pairs of hairs of various spacings and Re's are plotted in Fig. 5, which illustrates the following points:

(1) Appendages bearing hairs that operate at very low Re's are paddle-like with little fluid leaking between the hairs, whereas those whose bristles operate at Re's approaching one are much leakier and more rake-like. This suggests that many of the arrays of hairs on small organisms that biologists have described as sieves may in fact be functioning more like slightly leaky paddles. If such structures are involved in particle capture, they may do so by moving parcels of water containing particles

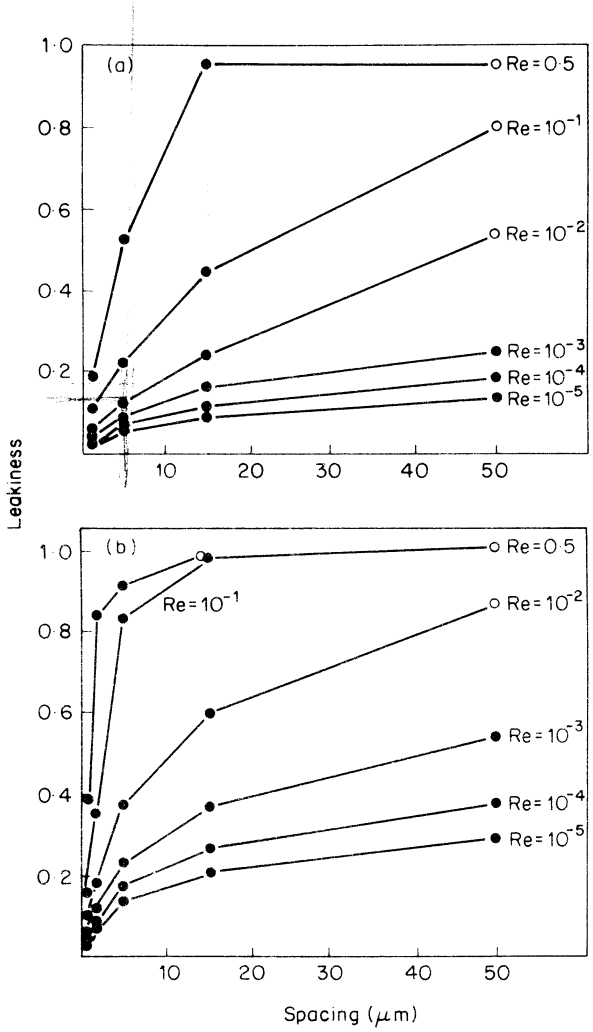

FIG. 5. Leakiness (defined in Fig. 4) of a pair of cylinders plotted vs. the width of the gap (spacing) between the cylinders. Numbers at the right end of each curve indicate the Re (based on cylinder diameter). Results for cylinders 1 μm in diameter are shown in (a), and for those 0·1 μm in diameter in (b). Flow profiles used for the points indicated by black circles were calculated as described in Appendix 1. Flow profiles used for points indicated by open circles were calculated using Lamb's solution for Oseen's approximation to the Navier-Stokes equations of motion (see Appendix 1).

rather than by straining the particles out of the fluid (as appears to be the case for certain feeding motions of calanoid copepods, Koehl & Strickler, 1981).

(2) A change in the Re of the motion of the hairs has little effect on leakiness at Re's of order 10^{-3} and smaller, and, for widely-spaced hairs, at Re's approaching 1. Therefore, we would expect that changes in speed would only be an effective mechanism of changing leakiness for organisms with fairly closely-spaced setae operating at Re's of about 10^{-2} and above.

(3) Changes in spacing between neighboring setae have the most pronounced effects on leakiness when the setae are already fairly close together. At Re's approaching 1, altering the width of the gap between widely-spaced hairs has no effect on leakiness; however, once the setae are moved close enough to "feel" their neighbors, further reductions in spacing cause a dramatic decrease in leakiness. The lower the Re, the smaller the effect on leakiness of changes in the spacing between hairs. (Note that we have not considered here separation in flow when two bodies are very close to each other (e.g. O'Neill, 1983); if eddies are thus formed in cases where hairs are very near to their neighbors, the leakiness should be even lower than we have predicted.)

(4) The slimmer the setae, the greater the leakiness for a given spacing and Re. This effect is most pronounced at Re's of order 10^{-3} and 10^{-2}.

Drag Force on Individual Hairs

The magnitude of the drag on a seta determines how much that seta deforms and whether or not it breaks when it is moved, and may represent a physical constraint on the behaviors available to an organism of a given morphology. Therefore, drag was calculated (as described in Appendix 1) for individual setae, both with a neighbor and when isolated. Although the drag coefficient of the hairs decreases, the drag force per unit length increases as Re increases (Fig. 6).

Our results point out some patterns in how the drag on a seta in a finite array is affected both by morphology and by speed of movement (Figs 7 and 8):

(1) When setae are far apart, their drag is the same as if they were isolated. However, drag on a seta is reduced as the spacing between neighbors is reduced. This drag reduction occurs because fluid is "traveling with" the neighbor, hence the velocity of that fluid with respect to the hair in question is less than it would be if the hair were alone. This result for a pair of setae is the opposite of that for the case of an infinite array of cylinders, in which the drag on a cylinder at a given free-stream velocity is increased as neighbors are moved closer and all the fluid must be forced through smaller spaces.

(2) A neighbor reduces drag by a greater proportion when the setae operate at lower Re's.

(3) At very low Re's a neighbor affects drag even when far away, whereas at Re's approaching 1, a neighbor must be very close to affect drag.

(4) Changing intersetal spacing has a bigger effect on the drag of setae that are already close together than on those farther apart.

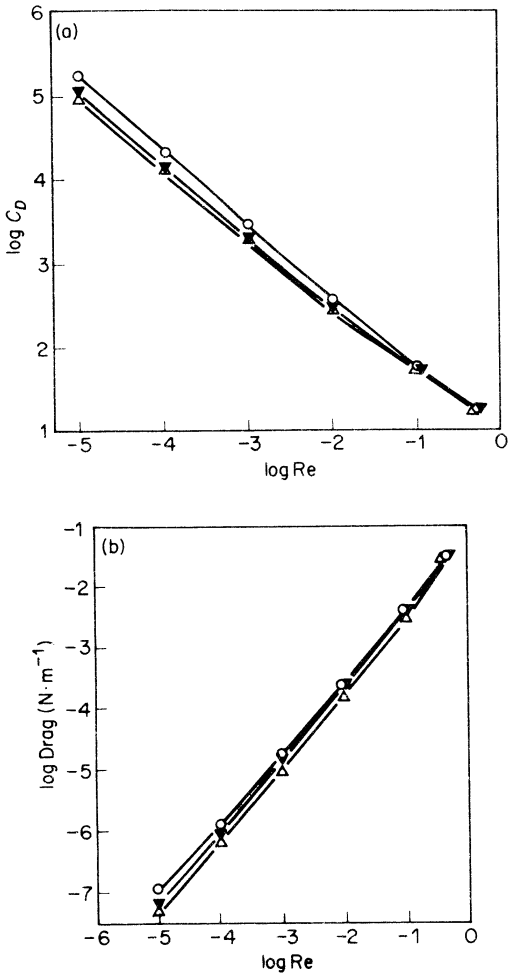

FIG. 6. (a) The log of the drag coefficient (C_D), and (b) log of the drag force per unit length of an isolated cylinder (○), and of a cylinder with a neighbor 50 μm away (▼) and 0·3 μm away (△), plotted vs. the log of Re. In this example, the cylinders are 0·1 μm in diameter.

(5) If setae are slim relative to the space between them, they must be closer together to "feel" the effect of neighbors on their drag at a given Re.

The results suggest that if an organism has closely-spaced setae in a row of finite width, it can get away with setae that are less stiff and strong than if it had them more widely spaced, especially at lower Re's.

The power requirement (and hence the energetic cost per time) for various behaviors by setulose appendages is a function of the force with which an organism must move those appendages. One might consider the force on the entire array of setae to be the sum of the forces on the individual setae. However, in cases where the setae are closely-spaced and the Re of the whole array is large enough that inertial effects on the array become important, such summing would not provide a good estimate of the force on the appendage. The work to move a bristled appendage

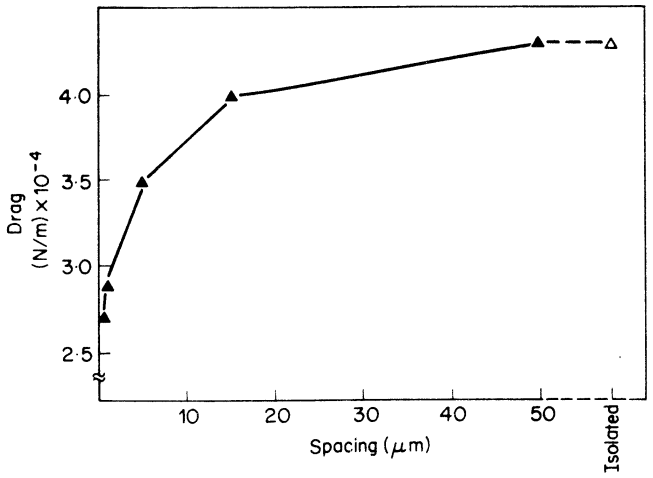

FIG. 7. Drag force per unit length on a cylinder plotted vs. the width of the gap (spacing) between it and the neighboring cylinder. The cylinders in this example are 0·1 μm in diameter and operate at a Re of 10^{-2}. Solid triangles (▲) represent a cylinder with a neighbor, and the open triangle (△) represents a cylinder with no neighbor.

might better be analyzed by considering the structure as a porous plate of finite width than by considering its individual setae as we have done here.

Discussion of Biological Implications

FUNCTIONAL MORPHOLOGY OF BRISTLED APPENDAGES

The steepness of the shear gradients near bristles and the leakiness of bristled appendages affect a number of biological processes, including: (i) the mechanisms by which such appendages can capture food particles (e.g. grabbing food vs. filtering vs. paddling water containing particles), (ii) the flux of dissolved substances to and from the surfaces of the hairs, and (iii) their performance while moving fluid to locomote or to create currents for respiration or feeding. Our results point out those aspects of the setae, bristles, and hairs of small organisms that are important to the flow around them. Our results can also be used to predict those circumstances under which particular changes in morphology or behavior are likely to affect, or to make little difference to, the performance of a finite row of hairs.

Although the width of the space between adjacent cylinders is perhaps the most often measured feature of rows of biological fibers, this morphological parameter alone is *not* an adequate predictor of the leakiness of such a structure for a small organism. The shear gradient next to a bristle depends primarily on the Re at which the appendage's bristles operate (that is, on the diameter and velocity of a bristle), but also on the ratio of the diameter of the hairs to the spacing between them. Therefore, it is critical to know the velocity at which setulose structures operate as well as to know their morphology if their function is to be interpreted. It is also important to consider the width of the row of bristles as well as the restrictions on

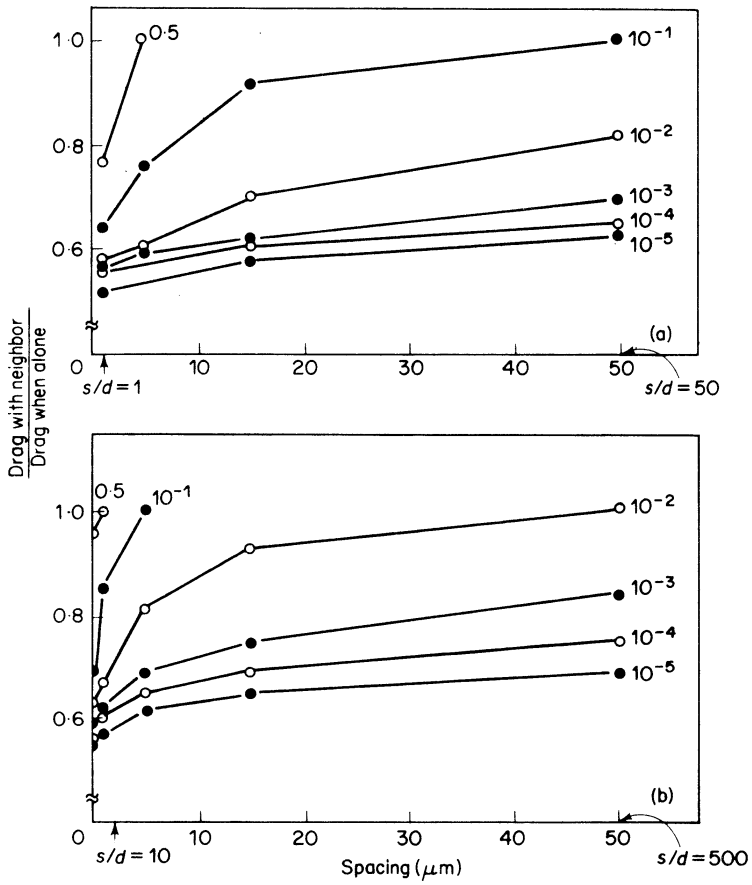

FIG. 8. Ratio of drag on a cylinder with a neighbor to drag on that cylinder when isolated, plotted vs. width of the space between neighbors. Results for a seta 1 μm in diameter are shown in (a), and for a seta 0·1 μm in diameter in (b). The ratio (s/d) of spacing between neighbors to cylinder diameter is indicated by arrows at selected spacings.

fluid motion caused by structures neighboring the appendage, as will be discussed below.

Our results should be kept in mind when considering the functional morphology of setulose appendages that are attached to the body at one end and hence sweep through an arc as they flap. As these appendages move, the distal ends of their setae travel at a greater velocity than do their basal ends; thus the distal ends not only have the potential of "processing" a greater volume of water per time, but also experience steeper shear gradients if the setal diameter and spacing are uniform base-to-tip. (Often setae are slimmer and more widely-spaced distally, both of which would further increase the leakiness of the distal portion of the appendage.) Thus, the performance by an appendage of any activity affected by shear gradient or leakiness is likely to be a function of position along the appendage. Different portions of an appendage that are morphologically identical may be quite different in function. Furthermore, portions of an appendage that look quite different from each other

may in fact be operating in a similar manner if the differences in structure compensate for the differences in velocity.

MECHANISMS OF INCREASING LEAKINESS

Because the effects of morphology on the flow through a finite array of cylinders is quite different from those on flow through an infinite row, it is important to know whether fluid can move around the edges of a row of hairs on an organism. When fluid is free to move around as well as through an array of hairs, shear gradients become less steep and drag on a hair is reduced as the width of the gap between the hairs is made smaller. In contrast, all the fluid is forced to move between the bristles in an infinite array, hence shear gradients become steeper and drag on individual bristles becomes higher as they are moved closer together. Therefore, especially in the case of closely-spaced setae, the performance of the setae can be changed if they are surrounded by structures that inhibit fluid movement around the perimeter of the array. This suggests that an organism might change the function of an appendage (for example from a swimming paddle to a particle-straining rake) by altering the neighborhood in which the appendage moves; such a switch in function might even occur as an appendage changes position within one cycle of flapping. No doubt, under certain conditions the width of a row of setae will affect the difficulty with which fluid can escape around the edges of the row, and hence will affect leakiness and drag. Although we point out the potential importance of this effect, we do not explore it quantitatively in this paper.

Arrays of hairs operating at low Re's can be made leakier than our model predicts by a number of mechanisms. In addition to placing flow barriers at the perimeter of a fibrous structure or to having a very wide row of hairs, other possible mechanisms of increasing the flow between the cylinders might be: (i) to draw fluid between the bristles by moving another structure away from the downstream side of the row of bristles (for example, perhaps this occurs when the first maxillae move away from the downstream side of the setulose second maxillae of a calanoid copepod, as described by Koehl & Strickler, 1981); and (ii) to push fluid between bristles by moving the bristles towards some other structure, such as another appendage or the surface of the body (perhaps this happens, for instance, when the second maxillae of a copepod do their "squeeze" motion, as shown in Koehl & Strickler, 1981). Of course leakiness-enhancing mechanisms also increase the drag on a hair operating at a given Re. Comparison of measured leakiness with that predicted by our model may prove useful for pointing out when leakiness-enhancing mechanisms are being used by an organism.

CHANGES IN FUNCTION DURING ONTOGENY OR EVOLUTION

The effects outlined above of differences in morphology or velocity on the water flow near setulose structures also apply to changes in size, shape, or speed of movement that occur through ontogenetic or evolutionary time. We suggest the Re's at which changes make little difference in performance versus those at which specific

changes have particular consequences. We hope these physical rules prove useful in future analyses of larval forms of and growth by bristled organisms, as well as in studies of evolutionary changes of such creatures.

As an organism increases in size, its Re increases unless it simultaneously lowers its velocity a concomitant amount. If growth carries an organism from very low Re's (where viscous forces predominate) to Re's of order one and above (where inertial effects become important as well), we would expect to find changes in the physical processes by which the organism deals with the fluid around it. For example, Batty (1984) describes how the swimming mechanisms of larval fish change as they increase in Re. Similarly, our results suggest that as bristled organisms (such as the setulose larvae of crustaceans) get bigger, their hairy appendages become leakier. Structures physically constrained to be paddles at small size acquire the potential to be strainers at larger size. Conversely, if setulose appendages are to remain paddles when big, gaps between setae should be filled in (for example, by setules or membranes). Furthermore, as the Re of paddles increase above 1, the role of inertia in the generation of propulsive force becomes greater; therefore, different physical rules become important in governing paddle performance.

Our suggestion that a novel function can accompany a simple change in the size of a bristled structure of a small organism may have evolutionary implications. Kingsolver & Koehl (1985), studying the evolution of wings in insects, have demonstrated an example of how an isometric change in the size of an animal can lead to a radically new function, and have suggested that this phenomenon might represent an important mechanism of evolutionary change. (In the case of insect protowings, function can change from thermoregulatory to aerodynamic, whereas in the case of the setulose structures considered here, function remains hydrodynamic as size increases, but paddles can become rakes.) If, as in these examples, a structure acquires a novel function, it is probably open to a new suite of selective pressures on its form. We suggest that further examination of biological phenomena involving fluid motion at Re's approaching one might prove a rich source of other examples of changes in mechanism of operation accompanying simple changes in size.

The same effects expected from an increase in size would also be expected from an increase in velocity, which likewise raises the Re. This effect of velocity suggests another possible avenue by which novel function can arise without requiring drastic changes in morphology.

This research was supported by N.S.F. (U.S.A.) Grants #OCE-8201395 and #OCE-8510834 to M. Koehl, and S.E.R.C. (U.K.) Grant #GR/D/13573 to J. D. Murray, whom we thank for the use of facilities at the Centre for Mathematical Biology, University of Oxford. We are grateful to N. Silvester for helpful comments and to an anonymous reviewer for suggesting inclusion of the material in Appendix 2.

REFERENCES

BRENDELBERGER, H., HERBECK, M., LANG, H. & LAMPERT, W. (1986). *Arch. Hydrobiol.* **107**, 197.
CHEER, A. Y. L. & KOEHL, M. A. R. (1987). *I.M.A. J. Math. Appl. Med. Biol.* **4**, 185.
CRAIG, D. & CHANCE, M. M. (1982). *Can. J. Zool.* **60C4**, 712.
DAVIES, C. N. (1973). *Air Filtration.* New York: Academic Press.

ELLINGTON, C. P. (1975). In: *Swimming and Flying in Nature Vol. 2.* (Wu, T. Y, Brokaw, C. J. & Brennan, C., eds). p. 783. New York: Plenum Press.
ELLINGTON, C. P. (1980). *J. Exp. Biol.* **85,** 129.
FENCHEL, T. (1980). *Limnol. Oceanogr.* **25,** 733.
FENCHEL, T. (1982). *Mar. Ecol. Prog. Ser.* **8,** 21.
GANF, G. G. & SHIEL, R. J. (1985). *Austr. J. Mar. Freshw. Res.* **36,** 371.
GAVIS, J. (1976). *J. Mar. Res.* **34,** 161.
GERRITSEN, J. & PORTER, K. G. (1982). *Science* **216,** 1225.
KAPLUN, S. (1957). *J. Math. Mech.* **6,** 595.
KAPLUN, S. & LAGERSTROM, P. A. (1957). *J. Math. Mech.* **6,** 585.
KINGSOLVER, J. G. & KOEHL, M. A. R. (1985). *Evolution* **39,** 488.
KOEHL, M. A. R. (1984). In: *Trophic Dynamics Within Aquatic Ecosystems.* (Strickler, J. R. & Meyers, D. eds). p. 135. New York: Westview Press.
KOEHL, M. A. R. & STRICKLER, J. R. (1981). *Limnol. Oceanogr.* **26,** 1062.
KUETHE, A. M. (1975). In: *Swimming and Flying in Nature, Vol. 2* (Wu, T. Y.-T., Brokaw, C. J. & Brennen, C., eds.). p. 803. New York: Plenum Press.
LAMB, H. (1911). *Phil. Mag. S. 6,* **21,** 112.
MCCLATCHIE, S. & BOYD, C. M. (1983). *Can. J. Fish. Aquatic Sci.* **40,** 955.
MIYAGI, T. (1958). *J. Phys. Soc. Japan* **13,** 493.
O'NEILL, M. E. (1983). *J. Fluid Mech.* **133,** 427.
OSEEN, C. W. (1910). *Ark. Math. Astronom. Fys.* **6,** 29.
PORTER, K. G., FEIG, Y. S. & VETTER, E. F. (1983). *Oecologia* **58,** 156.
PRICE, H. J. & PAFFENHÖFER, G.-A. (1986). *Limnol. Oceanogr.* **31,** 189.
PROUDMAN, I. & PEARSON, J. R. A. (1957). *J. Fluid Mech.* **2,** 237.
ROSS, D. H. & CRAIG, D. A. (1980). *Can. J. Zool.* **58,** 1186.
SILVESTER, N. R. (1983). *J. Theor. Biol.* **103,** 265.
SPEILMAN, L. A. (1977). *Ann. Rev. Fluid Mech.* **9,** 297.
STOKES, G. G. (1851). *Trans. Camb. Phil. Soc.* **9,** 8.
TAMADA, K. & FUJIKAWA, H. (1957). *Quart. J. Mech. Appl. Math.* **10,** 425.
UMEMURA, A. (1982). *J. Fluid Mech.* **121,** 345.

APPENDIX 1

Consider a circular cylinder of diameter D in steady translation motion, with speed U, through an otherwise undisturbed fluid of density ρ and dynamic viscosity μ. The inertial forces on the fluid are of order $\rho U^2/D$ and the viscous forces of order $\mu U/D^2$. The Reynolds number ($\mathrm{Re} = \rho UD/\mu$) is thus a measure of the relative importance of the viscous terms and the inertial terms in the equations of motion. The motion through water of the setae, bristles, or hairs of small organisms can be described by equations for flow at very small Re's.

The Navier-Stokes equations of motion and the respective boundary conditions for a cylinder moving in an infinite pool of water are:

$$(\mathbf{u} \,.\, \nabla)\mathbf{u} = -\nabla p + (1/\mathrm{Re})\,\Delta\mathbf{u}$$

$$\mathrm{div}\,\mathbf{u} = 0$$

$$\mathbf{u} = 0 \quad \text{on the boundary of the cylinder,}$$

where $\mathbf{u} = (u, v)$ is the velocity vector in two dimensions, p is the pressure, ∇ the gradient operator and Δ the Laplacian. When $\mathrm{Re} \ll 1$, Stokes (1851) reasoned that the viscous terms ($[1/\mathrm{Re}]\Delta u$) dominate while the convective terms ($[\mathbf{u} \,.\, \nabla]\mathbf{u}$) may be neglected. With this approximation, the above equations reduce to:

$$\nabla p = (1/\mathrm{Re}) \,.\, \Delta\mathbf{u}$$

$$\mathrm{div}\,\mathbf{u} = 0$$

$$\mathbf{u} = 0 \quad \text{on the boundary.}$$

The boundary condition at infinity (relative to the coordinate system fixed at the center of the body) is $\mathbf{u} = \mathbf{U}_\infty$, where $\mathbf{U}_\infty$ is the free-stream velocity far from the body.

The velocity distribution satisfying these Stokes equations and the no-slip boundary condition is given by:

$$\mathbf{u} = U_\infty + CU_\infty\{-(1/2)\log(r/a) - (1/4) + (1/4)(a^2/r^2)\}$$

$$+ Cx(U_\infty x/r^2)\{(1/2) - (1/2)(a^2/r^2)\},$$

where a is the radius of the cylinder, U_∞ the freestream velocity, r the distance from the center of the cylinder, and C a constant. However, there is no choice of the constant C that will satisfy the condition at infinity; Stokes' solution indicates that the quantity of fluid carried along with the moving cylinder increases indefinitely. Stokes reasoned that the inertial forces, which involve first order spatial derivatives, are insignificant relative to the viscous forces, which involve second order derivatives. However, upon examination of the magnitudes of these terms we see that the local inertia forces calculated from this solution are in fact comparable to the viscous forces when r is large. Although the above solution is not a self-consistent approximation of the flow field at large values of r, it is valid for small values of r (i.e. close to the cylinder).

Oseen (1910) proposed that the convective terms, rather than be neglected altogether, be approximated by their linearized forms, which are valid far from the cylinder where the difficulties with Stokes' approximation arise. He suggested that the Stokes equations be replaced by:

$$(1/\mathrm{Re})\Delta\mathbf{v} + (\mathbf{U}_\infty \cdot \nabla)\mathbf{v} = -1/\rho\,\nabla p$$

$$\operatorname{div}\mathbf{v} = 0, \quad \text{where } \mathbf{v} = \mathbf{u} - \mathbf{U}_\infty.$$

This amounts to linearizing the Navier-Stokes equations about $\mathbf{U}_\infty$ whereas the Stokes equations amount to linearizing them about $\mathbf{0}$.

Lamb (1911) gave a solution to Oseen's equations which showed that Oseen's approximation gave significant improvement at ∞, but was less accurate near the surface of the cylinder. Near the surface this solution only approximately satisfies the surface boundary conditions.

In order to obtain approximations for all values of r, one can employ the method of matched asymptotic expansion. For small Re's, let Stokes approximation be the leading term in an asymptotic expansion, which we shall call the Stokes expansion. Because of the limitations of Stokes' approximation mentioned previously, this series is not valid far from the cylinder where r is of order $O(1/\mathrm{Re})$. For the region far from the cylinder, a second asymptotic expansion is introduced which we call the Oseen expansion.

A uniformly valid composite expansion can be constructed by combining the Stokes expansion (which approximates the flow near the cylinder) with the Oseen expansion (which approximates the flow far from the cylinder). Since both of these expansions are approximations to the same Navier-Stokes equations of motion, it

is not unreasonable to impose that the two expansions must agree in some overlapping intermittent region (see Kaplun, 1957; Proudman & Pearson, 1957; Kaplun & Lagerstrom, 1957).

In this paper the velocity vector field around and the forces on two equal circular cylinders moving in a fluid of infinite extent is calculated using the matched-asymptotic analysis of Umemura (1982).

Consider the flow past two equal cylinders, each of radius a and at a distance d apart (Fig. A1). The resulting flow field between and around these two cylinders can be viewed as the flow past two setae in translational motion with speed U_∞ in a fluid of infinite extent. The mathematical problem consists of finding an approximate solution to the equations of motion satisfying the no-slip boundary condition on each cylinder and a uniform stream at infinity.

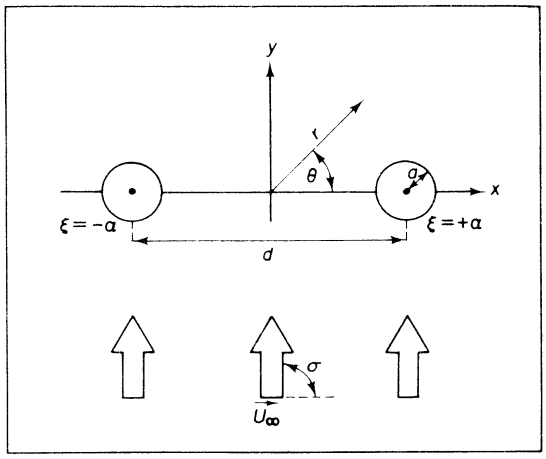

FIG. A1. Two-dimensional cross-section of a pair of cylinders of radius "a" whose centers are distance "d" apart. Free-stream velocity with respect to the cylinders (U_∞) is in the y direction and is indicated by the wide arrows.

To use matched asymptotic expansions the space around the cylinders is divided into two separate but overlapping regions, and an appropriate expansion valid in each region is considered. For the inner region close to the cylinders where $(\mathrm{Re})(r) \leq 0(1)$, the Stokes expansion is utilized. This inner expansion is valid asymptotically as $\mathrm{Re} \to 0$ for fixed r, and satisfies the no-slip boundary condition on both cylinders. Since the geometry of the problem affects the flow in this region, the appropriate coordinate system to represent the Stokes expansion will be the bi-polar coordinate system (ξ, η).

For the outer region where $(\mathrm{Re})(r) \geq 0(1)$, Oseen's expansion is utilized. This outer expansion takes inertial effects into consideration and is valid asymptotically as $\mathrm{Re} \to 0$ for a fixed value of r lying in the outer region. This expansion also satisfies the condition at infinity. Since flow far from the obstacle is less affected by the geometry, the Oseen expansion will be represented by the polar coordinate system (r, θ).

The inner and outer expansions must agree in an overlapping region where $(\mathrm{Re})(r) \sim 0(1)$. This matching condition will give the necessary boundary conditions to determine the constants in the expansion. Furthermore, in the overlapping region a transformation between the two coordinate systems is used so that both expansions are valid in this region. The flow field close to the cylinders (i.e. $[\mathrm{Re}][r] \leq 0[1]$), will be described by Stokes expansion in bi-polar coordinates, and the flow field far from the cylinders (i.e. $[\mathrm{Re}][r] > 0[1]$) will be described by Oseen's expansion in polar coordinates.

For the inner expansion the stream function is given by

$$\psi = \frac{c}{d} \frac{\phi}{\cosh \xi - \cos \eta}$$

where c and d are constants determined by the conditions $a = c \operatorname{cosech} \alpha$, and $d = 2 \coth \alpha$. Then ϕ is determined so that the stream function ψ satisfies the no-slip boundary condition on each of the cylinders:

$$\{\text{i.e.} \quad \partial\psi/\partial\eta(\pm\alpha) = 0, \quad \text{and} \quad \partial\psi/\partial\xi(\pm\alpha) = 0\}.$$

Hence,

$$\begin{aligned}\phi = P \Big[& \sinh \xi \ln (\cosh \xi - \cos \eta) + \hat{A}\xi(\cosh \xi - \cos \eta) + \hat{B} \sinh \xi \\ & + \sum_{n=1}^{\infty} \{\hat{b}_n \sinh (n+1)\xi + \hat{d}_n \sinh (n-1)\xi\} \cos n\eta \Big] \\ & - Q \Big[\sin \eta \ln (\cosh \xi - \cos \eta) \\ & + \sum_{n=1}^{\infty} \{\hat{a}'_n \cosh (n+1)\xi + \hat{c}'_n \cosh (n-1)\xi\} \sin n\eta \Big],\end{aligned}$$

where

$$\hat{A} = -\frac{2 + \cosh 2\alpha}{\sinh 2\alpha}, \qquad \hat{b}_n = \frac{1}{n} \frac{(n-1) - n\,\mathrm{e}^{-2\alpha} + \mathrm{e}^{-2n\alpha}}{n \sinh 2\alpha - \sinh 2n\alpha},$$

$$\hat{B} = \ln 2 - \alpha + \tfrac{3}{2} \coth \alpha, \qquad \hat{d}_n = \frac{1}{n} \frac{(n+1) - n\,\mathrm{e}^{2\alpha} - \mathrm{e}^{-2n\alpha}}{n \sinh 2\alpha - \sinh 2n\alpha},$$

$$\hat{b}_1 = -\frac{1 + 2\,\mathrm{e}^{-2\alpha}}{2 \sinh 2\alpha}, \qquad \hat{K} = -\frac{2 + \cosh 2\alpha}{\sinh 2\alpha} + \frac{3}{2},$$

$$\hat{a}'_1 = \frac{-1}{1 + \mathrm{e}^{2\alpha}}, \qquad \hat{a}'_n = \frac{1}{n+1} \frac{-(n+1) + n\,\mathrm{e}^{-2\alpha} + \mathrm{e}^{-2n\alpha}}{n \sinh 2\alpha + \sinh 2n\alpha},$$

$$\hat{c}'_1 = \ln 2 - \alpha - \tfrac{1}{2}\mathrm{e}^{-2\alpha} + \frac{\cosh 2\alpha}{1 + \mathrm{e}^{2\alpha}},$$

$$\hat{c}'_n = \frac{1}{n-1} \frac{-(n-1) + n\,\mathrm{e}^{2\alpha} - \mathrm{e}^{-2n\alpha}}{n \sinh 2\alpha + \sinh 2n\alpha},$$

and

$$\zeta = \frac{d}{2a} \quad \text{(non-dimensional distance between the axes of the two cylinders).}$$

P and Q are constants to be determined by the matching conditions.

The expansion in the outer region in polar coordinates is given by:

$$\Psi = G \sum_{n=1}^{\infty} \lambda_n(\tfrac{1}{2}r) r \frac{\sin n(\theta-\sigma)}{n} + H \sum_{n=1}^{\infty} \chi_n(\tfrac{1}{2}r) r \frac{\cos n(\theta-\sigma)}{n}$$

where: $\lambda_n = 2K_1 I_n + K_0(I_{n-1} + I_{n+1})$, and $\chi_n = K_0(I_{n-1} - I_{n+1})$. I_n and K_n are the Bessel function of the first and second kinds respectively of order n.

Upon matching the inner to the outer expansions, the multiplying factors P and Q are given by:

$$P = \frac{\frac{1}{2}(\ln R + \frac{1}{2} - g + q)\sin\sigma}{[\ln R - g + \frac{1}{2}(\tilde{p}+q)]^2 - \frac{1}{4}[(\tilde{p}-q)^2 + 2(\tilde{p}-q)\cos 2\sigma + 1]},$$

and

$$Q = \frac{\frac{1}{2}(\ln R + \frac{1}{2} - g + \tilde{p})\cos\sigma}{[\ln R - g + \frac{1}{2}(\tilde{p}+q)]^2 - \frac{1}{4}[(\tilde{p}-q)^2 + 2(\tilde{p}-q)\cos 2\sigma + 1]},$$

where σ is the angle at which U_∞ hits the cylinders (Fig. A1) ($\sigma = 90°$ in our calculations), and where

$$g = \tfrac{1}{2} - \gamma + 2\ln 2, \qquad \gamma = \text{Euler constant} = 0{\cdot}5772\ldots,$$

$$\tilde{p} = \ln(c/d) + \frac{1}{2}\left[\ln 2 - \hat{B} + \sum_{n=1}^{\infty}\{(n+1)\hat{b}_n + (n-1)d_n\}\right],$$

and

$$q = \ln(c/d) + \frac{1}{2}\left[\ln 2 + \sum_{n=1}^{\infty} n(\hat{a}'_n + \hat{c}'_n)\right].$$

After including the inertial effects and assuming that the flow can be expressed as a superposition of Φ and ϕ, we get:

$$\Phi = E_c \frac{\sinh\xi \sin\eta}{\cosh\xi - \cos\eta} + E_s \frac{\sinh^2\xi - \sin^2\eta}{\cosh\xi - \cos\eta},$$

where:

$$E_c = -\frac{3c}{16d}\cos 2\sigma, \qquad E_s = \frac{3c}{32d}\sin 2\sigma,$$

and

$$\phi = E_c\left[\hat{D}\xi \sin\eta + \sum_{n=1}^{\infty}\{\hat{b}'_n \sinh(n+1)\xi + \hat{d}'_n \sinh(n-1)\xi\}\sin n\eta\right]$$
$$+ E_s\left[\hat{\Gamma}(\cosh\xi - \cos\eta)\ln(\cosh\xi - \cos\eta)\right.$$
$$\left. + \hat{C}\xi\sinh\xi + \sum_{n=1}^{\infty}\{\hat{a}_n \cosh(n+1)\xi + \hat{c}_n \cosh(n-1)\xi\}\cos n\eta\right]$$

where:

$$\hat{D} = \frac{1-\cosh 2\alpha}{2\alpha\cosh 2\alpha - \sinh 2\alpha}, \qquad \hat{b}_1 = \frac{1-(1+2\alpha)\,e^{-2\alpha}}{2\alpha\cosh 2\alpha - \sinh 2\alpha}$$

$$\hat{b}'_n = \frac{-(n-1)+ne^{-2\alpha}-e^{-2n\alpha}}{n\sinh 2\alpha - \sinh 2n\alpha}, \qquad \hat{d}'_n = \frac{-(n+1)+n\,e^{2\alpha}+e^{-2n\alpha}}{n\sinh 2\alpha - \sinh 2n\alpha} \qquad (n \geqq 2)$$

$$\hat{C} = \frac{2}{2\alpha+\sinh 2\alpha} - \frac{2\sinh^2\alpha}{2\alpha+\sinh 2\alpha}\hat{\Gamma},$$

$$\hat{a}_1 = \frac{2}{e^{4\alpha}-1} + \frac{1}{e^{2\alpha}+1}\hat{\Gamma},$$

$$\hat{c}_1 = \frac{-4\alpha+4\sinh 2\alpha - \sinh 4\alpha}{2(2\alpha+\sinh 2\alpha)\sinh 2\alpha} + \frac{(2\alpha\cosh 2\alpha+\sinh 2\alpha)\sinh\alpha}{2(2\alpha+\sinh 2\alpha)\cosh\alpha}\hat{\Gamma}$$

$$\hat{a}_n = \frac{-(n-1)+n\,e^{-2\alpha}+e^{-2n\alpha}}{n\sinh 2\alpha+\sinh 2n\alpha} + \frac{1}{n(n+1)}\,\frac{(n+1)-n\,e^{-2\alpha}-e^{-2n\alpha}}{n\sinh 2\alpha+\sinh 2n\alpha}\hat{\Gamma}$$

$$\hat{c}_n = \frac{-(n+1)+n\,e^{2\alpha}-e^{2n\alpha}}{n\sinh 2\alpha+\sinh 2n\alpha} + \frac{1}{n(n-1)}\,\frac{(n-1)-n\,e^{2\alpha}+e^{-2n\alpha}}{\sinh 2\alpha-\sinh 2n\alpha}\hat{\Gamma}$$

and $\hat{\Gamma}$ is determined by the condition $\sum_{n=1}^{\infty}(\hat{a}_n + \hat{c}_n) = 0$.

The u and v velocities of the flow are obtained by applying the relationships $u = -\psi_y$ and $v = \psi_x$, where ψ is the stream function, $\psi_y = \partial\psi/\partial y$ and $\psi_x = \partial\psi/\partial x$. The derivatives ψ_y and ψ_x are approximated numerically by a second order finite difference formula.

The infinite sums needed to determine $\hat{\Gamma}$, ϕ, and Ψ are replaced by a finite sum. Since each successive term in these sums goes to zero exponentially, it is sufficient to include only the first five terms. The difference in the calculations of the stream functions between taking five and ten terms in the infinite sums is less than 10^{-7}.

The drag coefficient is given by

$$C_D = 8\pi(D\cos\sigma + C\sin\sigma)\zeta,$$

where $D = \hat{D}E_c$, $C = \hat{C}E_S$, and $\zeta = d/(2a)$. The drag force per unit length is given by:

$$\text{Drag} = aC_D U^2\rho$$

where a is the cylinder radius and ρ the density of the fluid.

For more details please refer to Umemura (1982).

APPENDIX 2

If bristled appendages are considered as porous plates, the flow through them might be estimated using Darcy's law. Approaches similar to this are given in examples such as Speilman and Goren (1968) and Silvester (1983). Other methods for estimating flow through and around screens submerged in fluid are given by Taylor & Batchelor (1949) and Koo & James (1973).

Let us consider an appendage consisting of a finite number (N) of equally-spaced cylinders (setae, bristles, etc.) each of diameter s. The flow through the appendage may be approximated by flow through a porous plate in the following way.

Let U_∞ denote the velocity of the flow passing around the appendage, L the width of the gap between the cylinders, l the width of the appendage ($l = N[L+s]+s$), and $\Lambda = L/s$ (Fig. A2). The velocity of the flow through the appendage is denoted by u. If u is small, then the flow field between the cylinders can be described by the solution to Stokes' equations. For a Stokes flow the drag F on each cylinder is approximately $\sim\mu us$ (leaving numerical constants aside), where μ is the viscosity of the fluid and u is the mean velocity of flow passing through the appendage. The net resistance per unit area of this appendage is thus approximately $F/\Lambda^2 s^2$, and the mean pressure gradient ∇p is approximately $s/\Lambda^3 s^3$. This says that Darcy's law may be used in the form

$$\mu us/\Lambda^3 s^3 \sim -\nabla p.$$

Solving for u we get

$$u \sim -\Lambda^3 s^2 \nabla p/\mu. \tag{1}$$

Substituting eqn (1) into the equations of continuity, we see that the pressure field satisfies the Laplacian. Upon taking the derivative with respect to l, we see that $\nabla p \sim p/l$. Substituting this back into eqn (1) we get:

$$u \sim [\Lambda^3 s^2 p]/\mu l. \tag{2}$$

The appendage Reynolds number (for flow around the entire appendage) is $R_1 = (U_\infty \rho l)/\mu$, where ρ is the density of the fluid. For the case where R_1 is small, the viscous forces are dominant and the pressure field is approximated by $p \sim \mu U_\infty/l$.

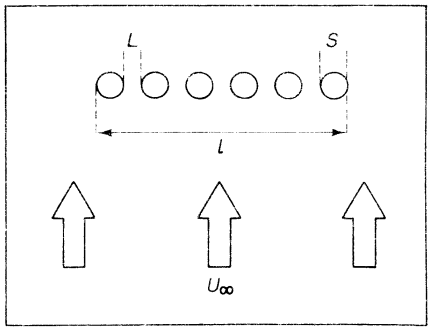

FIG. A2. Two-dimensional cross-section of an appendage of width "l" composed of cylinders of diameter "s" that are distance "L" apart. Free-stream velocity with respect to the appendage (U_∞) is indicated by the wide arrow.

For cases where R_1 is large, the inertial terms dominate in the flow and $p \sim \rho U_\infty^2$. This pressure field drives the flow through the porous plate. Substituting these terms into eqn (2) we obtain:

$$u/U_\infty \sim \begin{cases} L^3/sl^2 & \text{if } R_1 < 1 \\ L^3 R_1/dl^2 & \text{if } R_1 > 1. \end{cases}$$

The value u/U_∞ obtained using this approach is analogous to our "leakiness", as plotted in Fig. 5. For comparison, we have plotted u/U_∞ values calculated for an appendage composed of 20 setae with various setal diameters, intersetal spacings, and setal Reynolds numbers (Fig. A3). Although the results are qualitatively somewhat similar to those shown in Fig. 5, they are quantitatively comparable only for the 1 μm setae at Reynolds numbers of 10^{-3} and lower.

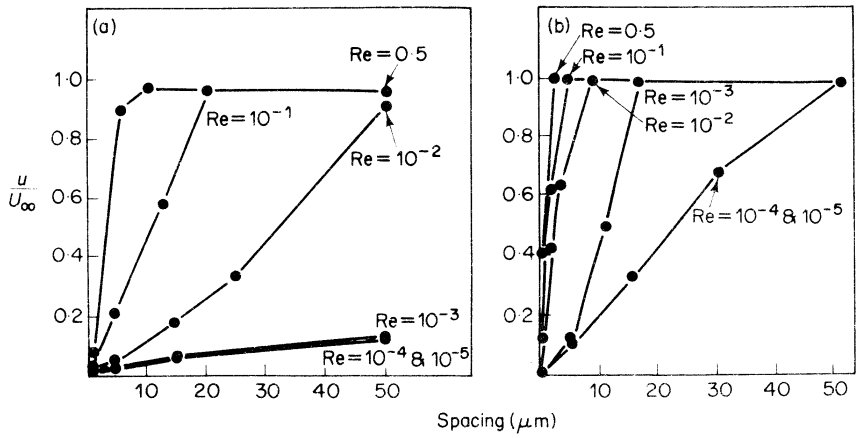

FIG. A3. Ratio of the velocity of flow through a porous plate (u) to the velocity of flow passing around it (U_∞) vs. the width of the gap (spacing) between the cylinders of which the plate is composed. Numbers at the right of each curve indicate the Re (based on cylinder diameter). Results for cylinders 1 μm in diameter are shown in (a), and for those 0·1 μm in diameter in (b).

Modeling a bristled appendage as a porous plate has the advantages of being a much simpler calculation than that described in Appendix 1, and of providing information about the effects of overall appendage width as well as of bristle morphology; it has the disadvantage of providing no description of the shear gradient next to the individual hairs in the appendage.

We have compared the predictions of the two-cylinder model and the porous plate model with empirical data for water flow through cephalic fans of aquatic black fly larvae. For this example, the two-cylinder model gives leakiness values that are 0·6 to 0·8 of measured values, whereas the porous plate model gives values that are 3×10^{-3} to 2×10^{-3} of measured values (Cheer & Koehl, 1987).

Therefore, we have chosen the two-cylinder model to be a more appropriate approximation for the biological questions addressed in this paper than the porous plate model, both because the former provides a description of the shear gradient next to individual bristles, and because the results of the former more closely approximate the biological data we have tested to date.